ELSEVIER

Ultramicroscopy 85 (2000) 9–13

ultramicroscopy

www.elsevier.nl/locate/ultramic

Ultramicroscopy Letter

Experimental characterisation of CCD cameras for HREM at 300 kV

R.R. Meyer[a], A.I. Kirkland[a,*,1], R.E. Dunin-Borkowski[b], J.L. Hutchison[b]

[a] *Department of Materials Science and Metallurgy, University of Cambridge, Pembroke Street, Cambridge CB2 3QZ, UK*
[b] *Department of Materials, University of Oxford, Parks Road, Oxford OX1 3PH, UK*

Received 23 January 2000; received in revised form 12 May 2000

Abstract

The modulation transfer function, noise transfer function and detection quantum efficiency of both $1k^2$ and $2k^2$ cameras attached to the same 300 kV FEGTEM have been measured. The results show that both the MTF and the DQE of the $2k^2$ camera are lower than for the $1k^2$ camera at frequencies above a third of the Nyquist limit. This lower per-pixel performance of the $2k^2$ camera is primarily a result of the use of a thicker phosphor scintillator. However, MTF and DQE of the $2k^2$ camera operated as an effective $1k^2$ camera by using 2×2 pixel binning are superior to the $1k^2$ camera in the medium spatial frequency range.

PACS: 07.78; 85.60.G; 42.30.L

Keywords: Charge-coupled device camera; Modulation transfer function; Detection quantum efficiency

1. Introduction

Charge-coupled device (CCD) cameras are increasingly replacing photographic film as the recording medium of choice in electron microscopy. One of their many merits is their linear response, which makes quantitative information available directly. For many quantitative applications that involve the measurement of information at different spatial frequencies, such as non-linear wavefunction reconstruction from focal series, it is essential to characterise the modulation transfer function (MTF) of the camera, which describes the attenuation of image contrast with spatial frequency [1–7]. It is equally important to measure the noise transfer function (NTF) of the camera [1], which describes the spatial frequency-dependent attenuation of the Poisson noise inherent in any electron image. We have previously found [1,2] that the NTF is substantially larger than the MTF at voltages of 200 kV and above. The noise method, which has been previously reported as measuring the MTF [3–5,7], thus overestimates the true MTF. This discrepancy between the MTF and the NTF results in a strong spatial-frequency dependence of the detection quantum efficiency (DQE) of the camera, which is a measure of the electron dose required to separate an image detail from noise.

*Corresponding author. Fax: +44-1223-446362.
E-mail address: aik10@cam.ac.uk (A.I. Kirkland)
[1] Also at: University of Cambridge, Department of Chemistry, Lensfield Road, Cambridge CB2 1EW, UK.

0304-3991/00/$ - see front matter
PII: S0304-3991(00)00046-2

In this letter, we describe the characterisation of, both the NTF and the MTF for a 1024×1024 pixel CCD camera and a 2048×2048 pixel CCD camera both coupled via nominally similar polycrystalline phosphor scintillators to the same 300 kV FEG-TEM. Differences between both the MTF and the NTF of the individual cameras are described and the experimental procedures used to measure them accurately are given.

2. Experimental MTF and NTF measurement

The MTF and NTF together with the corresponding DQE were measured for two CCD cameras that were both mounted on a JEOL JEM-3000F 300 kV field emission gun transmission electron microscope (FEG-TEM). In the first instance, a Gatan 794 Multiscan 1024×1024 pixel ($1k^2$) camera with a nominal pixel width of 27 μm, located immediately above the entrance aperture of a gatan imaging filter (GIF 2000) was used. The second device was a Gatan 794/IF20 Megascan 2048×2048 pixel ($2k^2$) camera with a nominal pixel width of 30 μm, located at the end of the GIF. Both the "upper" ($1k^2$) and "lower" ($2k^2$) cameras were equipped with proprietary polycrystalline scintillators fibre-optically coupled to the CCD-chips.

The MTF is most accurately measured using the edge method [3,4] which involves a sharp edge as an ideal test signal that contains all the spatial frequencies. This input signal includes frequencies beyond the Nyquist limit, and hence care must be taken to avoid aliasing artifacts. This can be achieved by using an edge that is inclined to the pixel columns [2]. In this geometry, an oversampled edge profile can be synthesised without interpolation by combining information from different rows of the image, as the position of the edge relative to the pixels varies from row to row. For n-fold oversampling, the edge positions in the individual linescans are aligned to a common origin with $1/n$ pixel accuracy and each linescan contributes to every nth pixel of the oversampled profile. The signal to noise ration (SNR) of this averaged edge profile is further improved by symmetrisation [2], leading to an excellent accuracy in the resultant MTF even at high spatial frequencies. In order to measure the MTF of the $1k^2$ camera, a rotatable aluminium insert containing a 1.2 mm thick knife-edge was placed onto the lower flange of the microscope photographic plate camera, with the edge positioned immediately above the CCD array (Fig. 1) (Al was used to minimise the generation of hard X-Rays near the CCD chip). The corresponding MTF of the $2k^2$ camera was measured by "jamming" the small retractable TV-rate CCD camera in the GIF by restricting the compressed air supply so that it obscured approximately half the field of view.

The NTF of each camera was measured from a series of 20 unprocessed images of uniform illumination [2]. After subtracting an average of 8 dark current images, the unprocessed images were then gain-normalised by division by the mean of the series. This also removes the effect of the illumination being slightly non-uniform. Subtracting the average of the previous and the next image from each processed image in the series effectively eliminated remaining non-noise contributions to the power spectrum due to drift in illumination conditions. The power spectra obtained were corrected for the effects of aliasing and pixel integration using an approach that has been described previously [2] and the NTFS (NTF corrected for sinc-function attenuation due to pixel integration) obtained as the rotational average of the corrected power spectrum. At very low spatial frequencies, the rotational average of

Fig. 1. The aluminium insert and knife edge used to measure the MTF of the $1k^2$ CCD camera.

the corrected power spectrum comprises only a few pixels; therefore, averaging over power spectra from many images was necessary to obtain reliable results at these frequencies. This averaging is essential for an accurate normalisation, for which the root of the noise power spectrum has to be extrapolated to zero spatial frequency.

For the upper camera, the gain was measured by imaging a small selected area aperture onto the CCD and measuring the beam current under these conditions with a Faraday cage. For the lower camera, the GIF entrance aperture was imaged onto the CCD and the beam current determined by measuring the GIF drift tube current with the sector magnet turned off.

For both cameras, the data required to determine the MTF and NTF were collected automatically using Digital Micrograph™ scripts, which are available from *http://www-hrem.msm.cam.ac.uk/~rrm/CCD/DM_Scripts*.

3. Results

Fig. 2(a) shows the MTFS (MTF corrected for sinc-function attenuation due to pixel integration [2]) for the $1k^2$ and $2k^2$ cameras and for the $2k^2$ camera operated in a 2×2 pixel binned mode. In all cases the plots extend to $k = \sqrt{(2)}/2$, which is the spatial frequency at each corner of Fourier space. The MTFSs are nearly identical in the low spatial frequency region, where back-scattering of electrons from the fibre-optic coupling is the dominant effect. At higher spatial frequencies, the MTFS of the $2k^2$ camera is poorer than that of the $1k^2$ camera, suggesting that the phosphor used in the $2k^2$ camera is substantially thicker than that in the $1k^2$ camera. An alternative explanation for the lower MTFS of the $2k^2$ camera is the possible surface curvature of the CCD chip leading to an imperfect coupling between the fibre plate and the CCD [8]. However, in this work this is unlikely to be significant as no variation in either the MTFS or NTFS was observed as a function of position within the chip. When the lower camera is used with 2×2 pixel binning, the MTFS is now superior to that of the upper camera. The results are summarised in Table 1.

For comparison, Fig. 2(b) shows the NTFS of each camera. The NTFS of the $2k^2$ camera decays more rapidly than that of the $1k^2$ camera at low spatial frequencies. It is also lower at high spatial frequencies, providing further evidence that the scintillator is thicker in the larger camera,

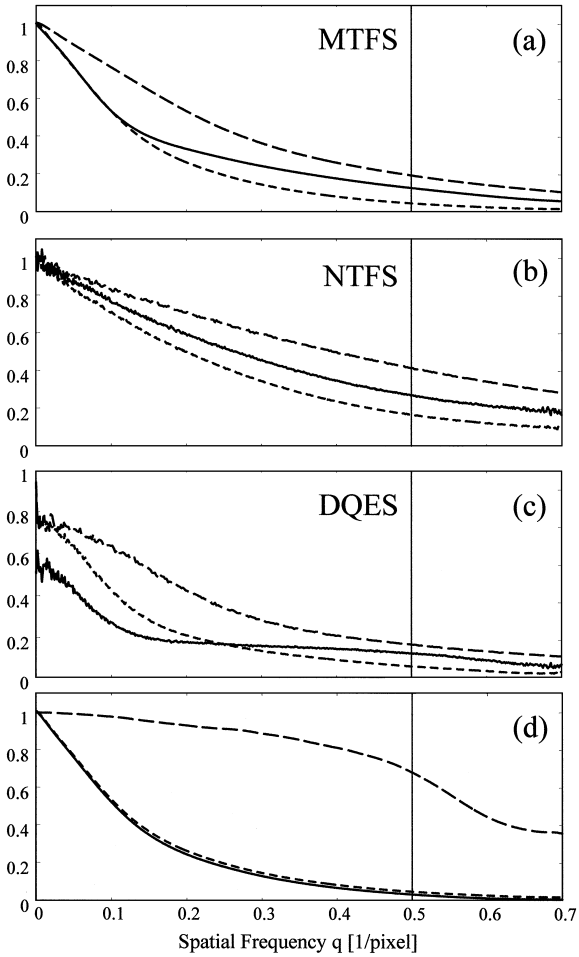

Fig. 2. (a) MTFS measured for the $1k^2$ and $2k^2$ cameras. Solid: $1k^2$, short dashed: $2k^2$, long dashed: $2k^2$ with 2×2 binning; (b) NTFS corresponding to (a); (c) DQE calculated from (a) and (b) using the values of G given in Table 1. In all cases plots extend from 0 spatial frequency to $k = (\sqrt{2})/2$, corresponding to the spatial frequency at the corner of Fourier space. In all plots the Nyquist frequency is marked. (d) MTFS calculated for the bottom camera using the upper Al insert as an edge (solid) compared to the MTFS with the retractable TV rate camera as an edge (short dashed). The ratio between the two is also shown (long dashed).

although the effect is much smaller than for the MTFS. This can be explained in the case of a thicker scintillator by the fact that the light generated close to the incident point (i.e. on the upper scintillator surface) provides the most accurate spatial information as it is unaffected by lateral electron scattering. However, as the fibre-optic coupling inevitably focuses onto the lower scintillator surface, this light in not imaged onto a point on the CCD chip, but onto an area with radius $t\tan(\alpha)$, where t is the scintillator thickness and α is the acceptance angle of the fibre-optic coupling. For phosphor scintillators, the phosphor grains are embedded in a matrix with $n = 1.2$ [9], which gives an acceptance angle of 55° when the fibre plate has a numerical aperture of 1. Furthermore, scattering and self-absorption in the phosphor makes it less likely that the light generated close to the upper surface can be detected, leading to a substantially more stringent requirement to use thin polycrystalline scintillators. Results from the NTFS determinations are also given in Table 1.

The gain G of the upper camera is measured as 4.5 DAC/e^- giving a zero spatial frequency DQE of 57%. The corresponding values for the lower camera are 16.6 DAC/e^- and 76%, respectively.

The spatial frequency-dependent DQE for the two cameras is shown in Fig. 2(c). Again, the DQEs are similar at low spatial frequencies but that of the $2k^2$ camera is lower at high spatial frequencies, as would be expected from the relative MTFSs and NTFSs. In all diagrams the spatial frequencies are given in units of pixel^{-1} and the graphs compare the per-pixel performance of the cameras, i.e. the DQE gives a comparator of the information content attainable with a certain electron dose in sub-images with the same number of pixels for both cameras.

For frequencies above a third of the Nyquist limit, the DQE of the $1k^2$ camera is substantially larger than that of the $2k^2$ camera, in spite of the 10% larger pixel size of the latter. This results from the thicker scintillator employed in the latter camera.

Fig. 2 also shows the MTFS, NTFS and DQE for the $2k^2$ camera operated with 2×2 pixel binning, effectively as a $1k^2$ camera with a pixel size of 60 μm. Compared to the conventional $1k^2$ camera, the DQE is improved for medium spatial frequencies.

We have also investigated the dependence of the DQE on the phosphor scintillator thickness using Monte-Carlo simulations [1,2]. These show that the high spatial frequency DQEs of phosphor scintillators can be improved substantially by using a thinner scintillator, but only at the cost of a slight reduction in the low spatial frequency DQE and a more substantial reduction in the gain.

The values given in Table 1 indicate that the $2k^2$ camera has a much higher gain then the $1k^2$ camera, which is again due in part to the thicker phosphor and in part to the higher gain of the pre-amplifier. As a thicker phosphor also improves the zero-spatial frequency DQE, the gain G is larger by a factor of 3.7 for the $2k^2$ camera compared with the $1k^2$ camera.

In order to confirm that the sharpness of the edges was sufficient for accurate MTF measurements, we have also investigated images of the

Table 1
Measurements of the MTFS, NTFS, DQE at 0 spatial frequency (0), Nyquist frequency (0.5) and half Nyquist frequency (0.25) and Gain

	MTFS(0.25)	MTFS(0.5)	NTFS(0.25)	NTFS(0.5)	Gain (G)
1k	0.29	0.13	0.52	0.27	4.50
2K	0.19	0.05	0.42	0.17	16.60
2k binned	0.44	0.19	0.65	0.42	16.60
	DQE(0)	DQE(.25)	DQE(.5)	DQE(.25)/DQE(0)	DQE(.5)/DQE(0)
1k	0.57	0.15	0.10	0.26	0.18
2K	0.76	0.15	0.05	0.19	0.07
2k binned	0.76	0.31	0.15	0.41	0.19

upper Al insert edge recorded with the bottom camera. Due to the ca. 20-fold magnification by the GIF, these images showed some edge roughness, with an average amplitude of about 1 pixel. Fig. 2d shows a comparison of the MTFS of the bottom camera measured from images of both the upper and lower edge. The MTFS obtained from the upper edge is lower at high spatial frequencies because the edge is not sufficiently sharp to be used with 20-fold magnification. However, the nearly perfect agreement of the graphs at low spatial frequencies shows that the relative error due to insufficient edge sharpness in the MTFSs obtained from unmagnified edge images is expected to be less than 1%.

4. Conclusions

We have measured the MTFS and NTFS at 300 kV for a $1k^2$ and a $2k^2$ CCD camera fitted to the same microscope both of which were coupled to phosphor scintillators via fibre-optic couplings. The results obtained indicate that, both the MTFS and the NTFS are lower for the latter, which is consistent with a thicker scintillator compensated partially by a larger pixel size. The DQE of the larger camera is higher at zero and low spatial frequencies but is lower at high spatial frequencies. The gain of the larger camera is 3.7 times larger than that of the small camera.

When the $2k^2$ camera is operated with 2×2 pixel binning, both the MTFS and the NTFS are improved beyond that of the $1k^2$ camera and the DQE is also improved significantly.

Acknowledgements

The authors are grateful to J. Stead for manufacturing the aluminium insert used and to R. Doole for assistance. Financial support from EPSRC and JEOL Ltd. (A.I.K.) is gratefully acknowledged.

References

[1] R.R. Meyer, A.I. Kirkland, Ultramicroscopy 75 (1998) 23.
[2] R.R. Meyer, A.I. Kirkland, Microscopy Research and Technique 49 (2000) 269.
[3] W.J. de Ruijter, J.K. Weiss, Rev. Sci. Instrum. 63 (1992) 4314.
[4] A.L. Weickenmeier, W. Nüchter, J. Mayer, Optik 99 (1995) 147.
[5] I. Daberkow, K.H. Herrmann, L. Liu, W.D. Rau, Ultramicroscopy 38 (1991) 215.
[6] J.M. Zuo, Proceedings of the 13th ICEM, Paris (1994) pp. 215.
[7] J.M. Zuo, Ultramicroscopy 66 (1996) 21.
[8] I. Daberkow, G. Lang, H.R. Tietz, Electron Microscopy 96, Proceedings EUREM 96 Vol. 1, 1996, 443.
[9] G.Y. Fan, M.H. Ellisman, Ultramicroscopy 52 (1993) 21.